Available online at www.sciencedirect.com
SCIENCE DIRECT®
Journal of Power Sources 135 (2004) 1–8
JOURNAL OF POWER SOURCES
www.elsevier.com/locate/jpowsour

^{7}Li NMR spectroscopy and ion conduction mechanism in mesoporous silica (SBA-15) composite poly(ethylene oxide) electrolyte

M. Jaipal Reddy, Peter P. Chu*

Department of Chemistry, National Central University, Chung-Li, Taiwan 32054

Received 27 January 2004; accepted 31 March 2004

Available online 19 June 2004

Abstract

A composite of mesoporous silica (SBA-15) with a polyethylene oxide (PEO) polymer electrolyte is examined for use in various electrochemical devices. Incorporation of SBA-15 in a PEO:$LiClO_4$ polymer electrolyte facilitates salt dissociation, enhances ion conductivity, and improves miscibility between organic and inorganic moieties. Optimized conductivity is found at 10 wt.% SBA-15 composition, above this concentration the conductivity is reduced due to aggregation of a SBA-15:Li rich phase. Heating above melt temperature of PEO allows more of the polymer segments to interact with SBA-15. This results in a greater degree of disorder upon cooling, and the ion conductivity is enhanced. A ^{7}Li MAS NMR study reveals three types of lithium-ion coordination. Two major types of conduction mechanism can be identified: one through conventional amorphous PEO; a second via hopping in a sequential manner by replacing the nearby vacancies ('holes') on the surface (both interior and exterior) of the SBA-15 channels.

Keywords: Composite polymer electrolyte; Poly(ethylene oxide); SBA-15; Ion conductivity; ^{7}Li NMR spectroscopy

1. Introduction

Considerable interest in solid polymeric electrolytes has been stimulated by their potential application in various electrochemical devices, such as high-energy secondary batteries, fuel cells, and sensors [1–3]. The structure and transport properties of these materials are closely related to their local configuration in the nearby coordinated cations. The presence of a salt not only provides a source of ions but also raises the glass transition temperature, T_g, and induces higher amorphous fraction. In general, this increases the conductivity but at high concentrations of salt ion-paring begins to form, which degrades conductivity and mechanical stability [4–7].

Any modifications should take into account of all possible ion–ion interactions that may exist in the system.

Various methods have been proposed to modify the polymer host matrix with the aim to improve electrolyte utility, e.g., adding plasticizers [8–12], dispersion of inorganic oxides, such as nano-sized TiO_2 [13,14], Al_2O_3 [14], SiO_2, fumed silica [15–18], and ceramic powders [11,16–23]. The addition of liquids as plasticizers raises the conductivity but the electrolyte mechanical properties suffers and the reactivity towards anode (i.e. lithium metal) heightens [8]. A favourable approach is to disperse nano inorganic oxide in a polymer substrate [13,14]. Prior studies have concluded that a composite electrolyte delivers better mechanical strength, higher ionic conductivity, and good anode|electrolyte interfacial contacts [13–23]. Lewis acid–base interaction satisfactorily accounts for the formation of numerous inorganic–polymer electrolyte composites [24–26]. According to such interaction, inorganic surface groups provide physical cross-linking centres for the polymer electrolyte (e.g., poly(ethylene oxide), PEO) and anions, thus reduce the polymer reorganization tendency. Additionally, the filler surface groups of the inorganic solid oxide form an ion–filler complex. The major conduction path is still originates from local diffusion within the amorphous polymer region, but additional transport can be established from the ion–filler complex.

In this paper, we explore modification of a PEO polymer with a different inorganic system that has a tubular nano-scale channel structure. SBA-15 is an inorganic oxide material in the form of mesoporous silica molecular sieves with uniform, long, connecting tubular channels of variable pore size from 5 to 30 nm and a large surface area [27]. The high surface area can facilitate uniform dispersion

* Corresponding author. Tel.: +886 34258631; fax: +886 34227664.
E-mail address: pjchu@cc.ncu.edu.tw (P.P. Chu).

0378-7753/$ – see front matter © 2004 Elsevier B.V. All rights reserved.
doi:10.1016/j.jpowsour.2004.03.078

in the polymeric matrix to yield more mobile ion species with a greater degree of salt dissociation through the formation of an ion–solid oxide complex. The loading of cations, such as Ti [28], Al [29] and V [30] in the channels of the mesoporous SBA-15 have been reported. Imperor-Clerc et al. [31] have reported that the structure of silica walls is more complex and show a 'corona' region of lower density around the cylindrical organic aggregates. Previous studies [32] confirmed that a PEO and mesoporous MCM-41 composite exhibits good inter-phase interaction (i.e. miscibility) in presence of a lithium salt through the penetration of both polymer and lithium ions within the pores of mesoporous silica [32]. These unique structure features are expected to induce changes in both the physical properties and the ion-conducting behaviour. This paper presenets a study of the crystallinity, coordination structure and transport mechanism of a lithium composite PEO polymer electrolyte with SBA-15 (SiO_2) as filler.

2. Experimental

Composite solid polymer electrolyte (CSPE) films were prepared by using poly (ethylene oxide) (PEO) [mol. wt. $= 2 \times 10^5$, Aldrich], a $LiClO_4$ salt in a (90:10) wt.% [Li/EO (1:21.7)] blend, and different weight percentages of SBA–15. Initially, the PEO was dissolved in tetrahydrofuran (THF) followed by the addition of appropriate amounts of $LiClO_4$ and SBA-15 in 2 h intervals and stirring for 24 h at 60 °C. The homogeneous mixtures were poured into Teflon dishes and evaporated slowly at 40 °C in a vacuum. Further drying was conducted in a dry-box under a nitrogen atmosphere to remove the solvent completely. All the samples were stored in a dry-box with a nitrogen atmosphere for protection from moisture.

The surface morphology of these composite electrolytes was studied by means of scanning electron microscopy (SEM) using a Hitachi [Model 3500N] instrument and gold-sputtered coated films. Differential scanning calorimetry (DSC) studies were performed in the temperature range of 30–100 °C with a Perkin-Elmer (DSC 7 series) system at a heating rate of 5 °C per min. Sample weights were maintained in the range of 5–6 mg and all experiments were carried out under a flow of nitrogen.

Impedance spectroscopy was used to determine the ionic conductivity of the polymer composite films. Measurements were performed over the frequency range of 1 MHz to 10 Hz, by means of a frequency analyzer AUTOLAB/PGSTAT 30 (potential/galvanostat) electrochemical instrument under a nitrogen environment. These measurements were made over the temperature range 298–373 K, and the system was thermally equilibrated at each selected temperature for 20 min. The bulk resistance (R_b) was determined from the equivalent circuit analysis by using Frequency response analyzer (FRA) software (less than 1% error). The conductivity values (σ) were calculated from the equation $\sigma = (l/R_b)\ (t/A)$, where t is the thickness and A the area of the sample.

Solid-state ^{7}Li magic angle spinning (MAS) NMR spectra were recorded on a Bruker DSX-300 spectrometer, operating at a resonance frequency of 116.6 MHz for the ^{7}Li nucleus. A spinning speed of 2 kHz was employed, which sufficiently removed the small shift anisotropy side-bands to avoid major complications.

3. Results

3.1. Morphology and crystallinity

Electron micrographs of pure PEO and PEO:$LiClO_4$ with SBA-15 are presented in Fig. 1. It is seen that PEO is a semi-crystalline polymer with a rough surface of several crystalline domains (Fig. 1(a)) [32]. On blending with lithium salt, the PEO surface morphology changes severely from rough to smooth (See Fig. 1(b)). For further modification, SBA–15 is incorporated in the PEO:$LiClO_4$ electrolyte matrix. The SBA-15 causes a marked change in the PEO:$LiClO_4$ morphology, see Fig. 1(c) and (d). At lower compositions, SBA-15 is dispersed homogeneously in the PEO:$LiClO_4$ electrolyte matrix. The lithium ions form Lewis acid–base interactions with both the inorganic solid oxide surface groups, while the ether oxygen of the PEO chain establishes the interaction for miscibility. Above 10 wt.% of SBA-15 composition, however, severe aggregated phases can be detected. The aggregated domains may correspond to mesoporous silica with Li ions [32].

The relative percentage of the crystalline (χ) form of the composite, has been calculated from DSC data, which are referenced to pure PEO being 100% crystalline, and from the equation $\chi = \Delta H_f / \Delta H_f^\circ$. DSC endothermic curves of the SBA-15 composite PEO electrolyte are displayed in Fig. 2. The DSC melting endothermic indicates reduction of PEO crystallinity in the presence of the lithium salt and this effect is enhanced with the addition of SBA-15, but complete depression of ΔH_f is not identified. The calculated relative crystalline data are summarized in Table 1. Both SEM and DSC investigations confirm that PEO crystallinity is reduced severely with addition of lithium salt and this is further by the presence of mesoporous oxide.

3.2. Ion conductivity

The isothermal characteristic conductivity of a SBA composite PEO electrolyte is shown in Fig. 3, and the conductivity data are summarized in Table 1. The ion conductivity increases with the oxide content and optimum value is found at 10 wt.% SBA-15 with one order of improvement over PEO:$LiClO_4$ SPE. In the case of 15 wt.% SBA, the conductivity is degraded but still half an order larger than that of pure PEO:$LiClO_4$ SPE. As shown by SEM and DSC studies, the organic–inorganic miscibility is better at

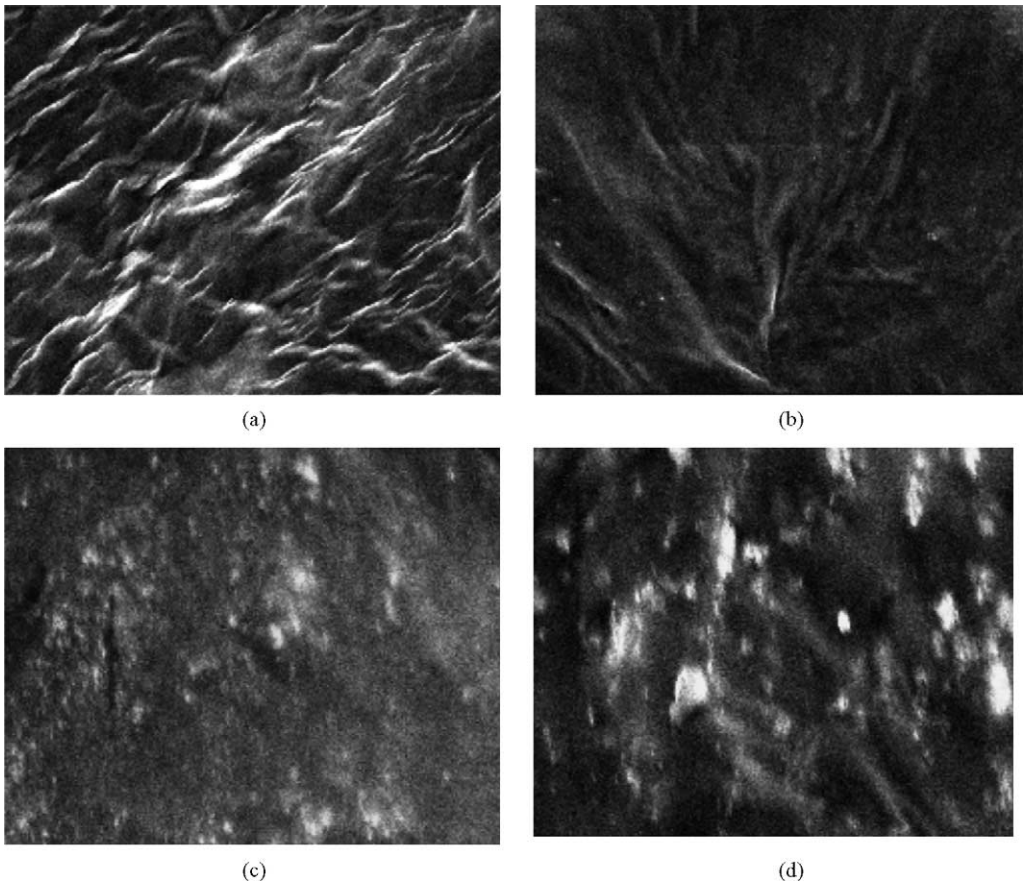

Fig. 1. Electron micrographs (×1500) of: (a) pure PEO; (b) PEO:$LiClO_4$ (90/10); (c) 5 wt.% and (d) 10 wt.% SBA-15 in PEO:$LiClO_4$ (90:10) polymer electrolyte.

Table 1
Crystallinity (χ), conductivity (σ) and activation energies of PEO:$LiClO_4$:SBA-15 composite solid polymer electrolyte system

SBA-15 (wt.%)	Si/Li	χ (%)	Conductivity (σ) (S cm^{-1})	Activation energies (E_a) kJ/mole	
				Region-I	Region-II
0	0	49.02	4.54×10^{-6}	36.7	12.2
5	0.89	34.8	6.98×10^{-6}	31.8	14.9
8	1.42	30.4	1.19×10^{-5}	30.9	15.4
10	1.77	31.4	2.62×10^{-5}	26.1	12.3
15	2.66	39.1	1.18×10^{-5}	30.8	13.7

Region-I: below melting temperature (T_m); Region-II: above melting temperature (T_m). χ (%): crystallinity with respect to pure PEO as 100%.

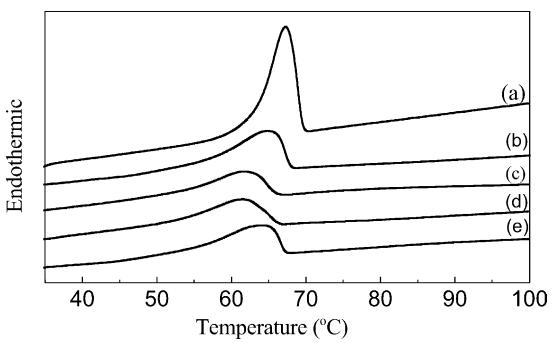

Fig. 2. DSC curves of (a) pure PEO; (b) 0; (c) 5; (d) 10 and (e) 15 wt.% of SBA-15 in PEO:$LiClO_4$ polymer electrolyte.

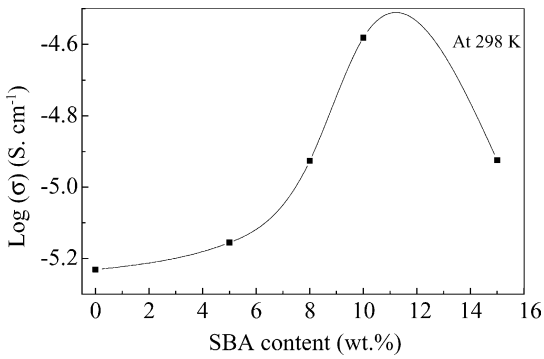

Fig. 3. Isothermal ion conductivity of SBA-15 composite PEO:$LiClO_4$ solid polymer electrolyte system at ambient temperature.

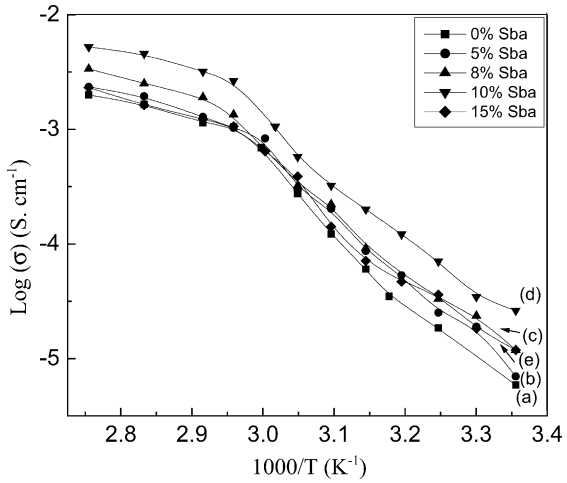

Fig. 4. Variable temperature conductivity of (a) 0; (b) 5; (c) 8 and (d) 10 and (e) 15 wt.% of SBA-15 in PEO:$LiClO_4$ polymer electrolyte.

inter-medium compositions but aggregation of larger mesoporous lithium-rich domains occurs at a composition above 10 wt.% SBA-15.

The effect of temperature (T) on the conductivity (σ) of a SBA-15 composite PEO:$LiClO_4$ is shown in Fig. 4. A sharp increase occurs at the PEO melting temperature (T_m). This is due to an increase in the amorphous domain, which is a typical characteristic of PEO electrolytes [32–38]. The Log (σ) versus 1000/T plots can be explained by different models of polymer electrolytes. The composite electrolyte studied here follows an Arrhenius-type, thermally activated, process below and above T_m. In both regions, the conductivity relationship can be expressed as:

$$\sigma = \sigma_0 \exp\left(\frac{-E_a}{kT}\right) \quad (1)$$

where σ_0, E_a, k are the pre-exponential factor, the activation energy and the Boltzman constant, respectively. The activation energies of the composite polymer electrolyte were evaluated by fitting the above equation to both the regions. The results are summarized in Table 1. The activation energies measured for both regions are different. It is noted that, in the low-temperature region, the activation energies of the composites are all smaller than that of a pure PEO:$LiClO_4$ electrolyte. The enhanced ionic conductivity and decrease in activation energies suggest a different ion transport behaviour in the composite.

The conductivity of this composite electrolyte follows different trends upon heating and cooling, see Fig. 5(a) and 5(b) that present the conductivity during heating and cooling of 10 and 15 wt.% SBA-15 composition polymer electrolyte films. On heating, the conductivity follows the typical behaviour for a polymer electrolyte with a marked increase near the PEO melting temperature. On subsequent cooling, the conductivity remains consistently higher compared with that during heating. The break in conductivity occurs between 35 and 45 °C, i.e. near the

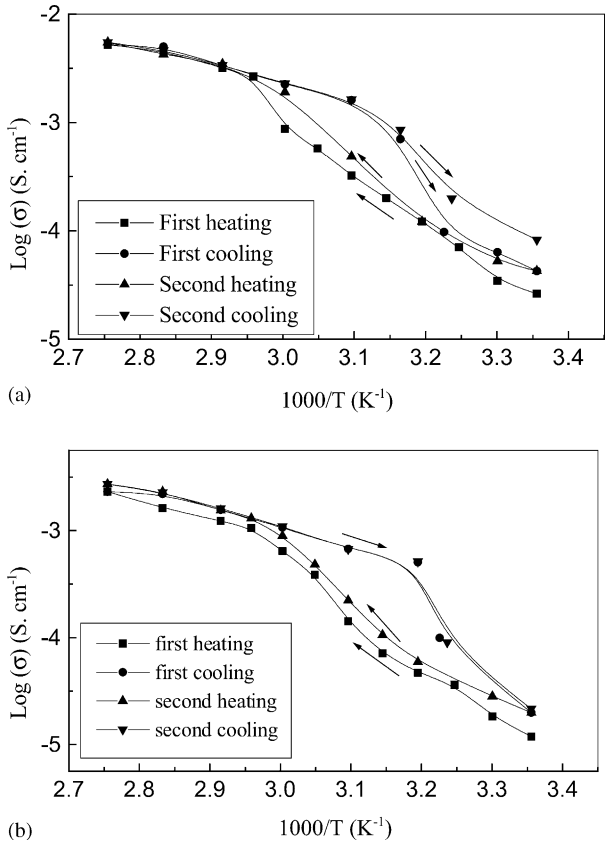

Fig. 5. (a) A variable temperature conductivity in two scans while heating and cooling for 10 wt.% of SBA-15 in PEO/$LiClO_4$ polymer electrolyte, (b) Variable temperature conductivity in two scans while heating and cooling for 15 wt.% of SBA-15 in PEO/$LiClO_4$ polymer electrolyte.

crystallization temperature (T_c), when cooling the sample [32,39].

For the 10 wt.% SBA-15 composite, the conductivity after annealing above the PEO melting temperature is two orders of magnitude larger than the pure PEO:$LiClO_4$ polymer electrolyte. In the case of the 15 wt.% SBA-15 composite, however, the difference is less pronounced. Note that, the 10 wt.% SBA-15 composite shows better miscibility, but a 15 wt.% SBA-15 composite exhibits more severe phase separations. It is likely that the conductivity discrepancy when heating and cooling is attributed to a reduction in PEO crystallization in presence of the filler when the composite electrolyte is annealed above the PEO melting temperature.

3.3. ^{7}Li *MAS NMR Spectroscopy*

^{7}Li MAS NMR spectra of the SBA-15 composite polymer electrolyte system are depicted in Fig. 6. NMR spectra of a SBA-15 composite PEO (Fig. 6(b) to (d)) with reference to the spectra of PEO:$LiClO_4$ (Fig. 6(a) reveal the emergence of shoulder peaks and line-width broadening with increasing SBA-15. At a high content (15 wt.%) of SBA-15, the ^{7}Li peak exhibits a most prominent shift compared with a PEO:$LiClO_4$ polymer (Fig. 6(d)). It is relevant

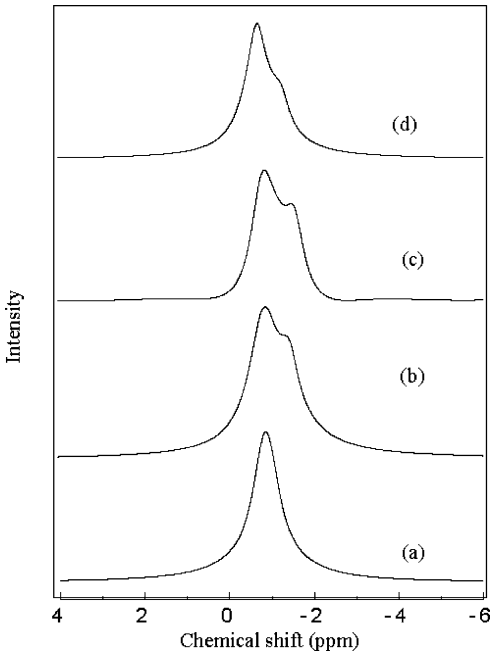

Fig. 6. ^{7}Li MAS NMR spectra of (a) 0; (b) 5; (c) 8; and (d) 15 wt.% of SBA-15 in PEO:$LiClO_4$ polymer electrolyte.

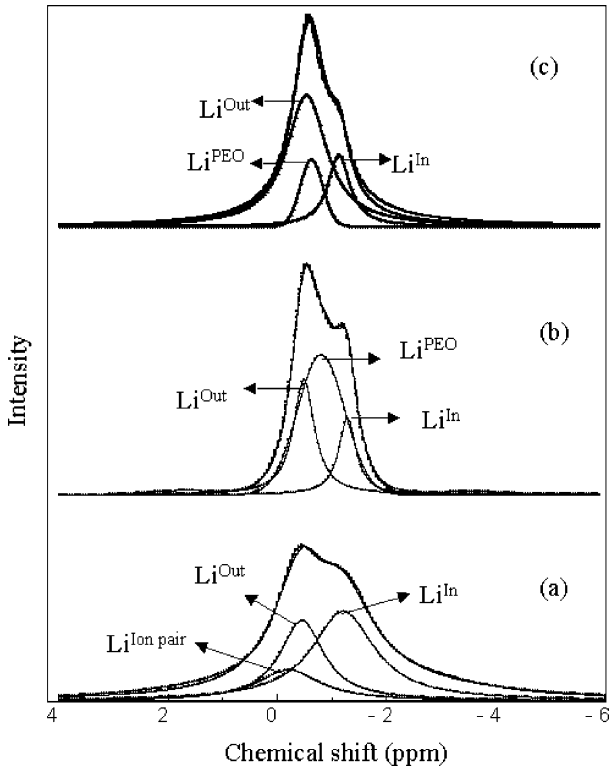

Fig. 7. Least square peak fits of ^{7}Li NMR spectra of (a) SBA-15:$LiClO_4$ (1:1 wt.%); (b) 8 and (c) 15 wt.% of SBA-15 in PEO:$LiClO_4$ polymer electrolyte.

and reasonable to assume that mesoporous composite polymer electrolyte exhibits at least three unique lithium species for coordination [32]. By virtue of its large pore channels, SBA-15 can upload larger cations, such as Ti [28], Al [29], V [30], etc. Lithium ions are smaller in size and can penetrate the pore channels and also coordinate on the surface of SBA-15. It is assumed that the three environments are: lithium species on the outer surface of SBA-15; lithium species in the interior pore channels of SBA-15; lithium species within the amorphous PEO. In the absence of PEO, ^{7}Li MAS NMR spectra of SBA-15:$LiClO_4$ (1:1 wt.% ratio) are given in Fig. 7(a).

The spectra of SBA-15:$LiClO_4$ have an asymmetrical shape with a broad width; which can be resolved into three peaks corresponding to the three lithium positions. Least-square decomposition by Lorentzian and Gaussian components reveals the characters of these components. In Fig. 7(a), the down-field peak '$Li^{Ionpair}$' (near ~ 0.0 ppm) is conveniently assigned to Li species of un-dissociated salt, and the two up-field peaks at middle 'Li^{In}' and higher 'Li^{Out}' are reasonably assigned to lithium ions that are coordinated on the outer surface and the interior channel of SBA, respectively. This result reveals a close interaction between lithium ions and mesoporous silica (SBA-15).

The results for SBA-15:$LiClO_4$ (1:1 wt.%) provide clear evidence that the SBA-15 composite polymer electrolyte bears three kinds of lithium coordination. The superimposed least-square peak fits with the raw data of 8 and 15 wt.% of SBA in PEO:$LiClO_4$ electrolyte are demonstrated in Fig. 7(b) and 7(c), respectively. The peak fits are signed as sites 'Li^{Out}', 'Li^{In}', and 'Li^{PEO}' where: site 'Li^{Out}' represents the lithium species on the outer surface (0.5–0.7 ppm); site 'Li^{In}' represents the lithium species inside the pore channels (1.1–1.5 ppm) of SBA-15, as previously assigned; site 'Li^{PEO}' represents lithium species with amorphous PEO (0.8–1.0 ppm). The lithium species with a SBA-15 content show an interesting trend: components of 'Li^{Out}' and 'Li^{In}' increases dramatically and 'Li^{PEO}' decreases with increase of SBA-15 in PEO:$LiClO_4$. This analysis indicates that lithium favours association with SBA-15 rather than PEO, since stronger Li:SBA-15 peaks develop with increase in SBA-15 content.

The ^{7}Li NMR line-width and relative population of the three major lithium conformations are summarized in Fig. 8(a) and 8(b), respectively, with curves 'Li^{out}', 'Li^{In}', and 'Li^{PEO}'.

The line-width and population of sites 'Li^{Out}' and 'Li^{In}' increase and those of site 'Li^{PEO}' decrease with increasing SBA-15 content. Interestingly, the combined intensity ratio of sites 'Li^{Out}' and 'Li^{In}' are approximately equal to site 'Li^{PEO}' when the content of SBA-15 reached 10 wt.%. Further increase of SBA-15 leads to a shift of lithium-ion population into the SBA-15 regime and a significant decrease in the polymer PEO. This confirms that lithium bears stronger association with mesoporous structured SiO_2 to raise the possibility of a marked development of a SBA-15:Li rich phase at higher SBA-15 compositions. These results corroborate with the SEM, DSC and conductivity measurements

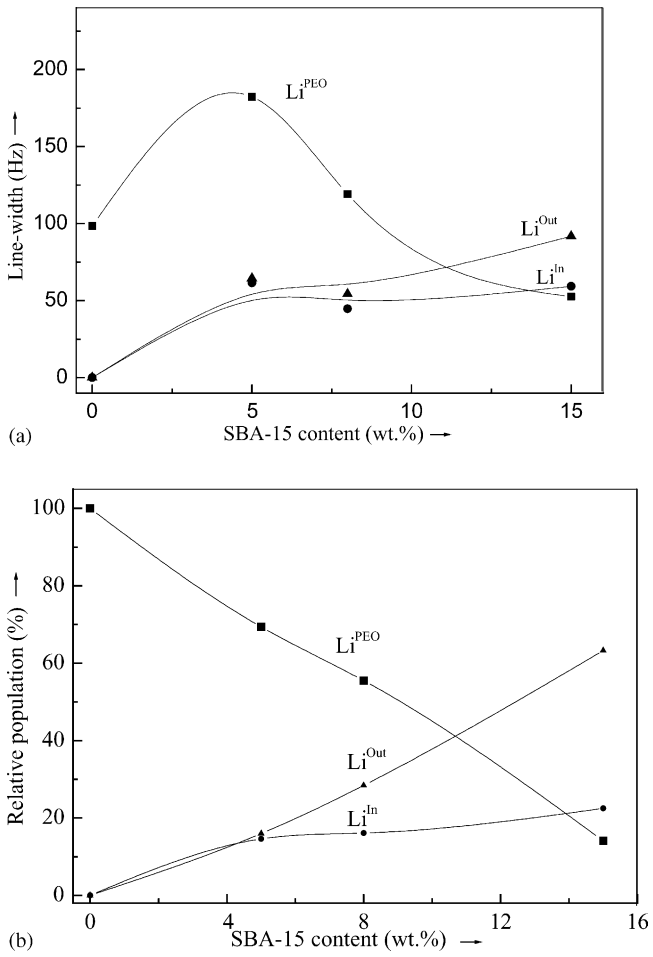

Fig. 8. (a) ^{7}Li NMR line-width variation of three components in PEO:$LiClO_4$:SBA-15 composite polymer electrolyte with a function of SBA-15; (b) ^{7}Li NMR relative population of three components in PEO:$LiClO_4$:SBA-15 composite polymer electrolyte with a function of SBA-15.

in which a larger SBA-15:Li rich aggregation phase is observed.

4. Discussion

SEM, DSC, ^{7}Li NMR, and conductivity studies confirm that SBA-15 composite PEO complex formation is highly induced in the presence of a lithium salt where the acid–base reactions enhances the compatibility of the organic and inorganic moieties. The NMR results show a stronger association of lithium ions with SBA-15 than with polymer PEO. It is interesting that SBA-15 has larger channel dimensions that favour occlusion of the PEO polymer along with the shift of lithium ions into the interior pore channels of SBA-15. The oxygen atoms in polymer PEO and mesoporous SBA-15 serve as Lewis base centres, and the Li^+ cation serves as a strong Lewis acid. Possibly, silica in SBA-15 is acting as a Lewis acid centre for physical cross-linking by weak electrostatic interaction with the base centre of the ether oxygen of the polymer PEO. This electrostatic interaction drives the occlusion of PEO and Li^+ ions into shallow channels. According to Wieczorek and co-workers [41,42], the Lewis acid of the added oxide filler would compete with the Lewis acid character of the lithium cations to form new complexes with the PEO chains. Thus, the filler oxide acts as cross-linking centres for the PEO chains. Such behaviour lowers the polymer reorganization tendency and promotes an overall mechanically-stable structure. The structure modification provides new lithium ion conduction pathways on the filler surface and is a salient feature that enhances ion transport. Wong et al. [43] reported that the interactions of polymer and cations with surface oxygen atoms occur in the silicate layer. The occlusion of polymer PEO in the pore channels of SBA-15 is plausible where the silica and ether oxygen of polymer can interact with weak electrostatic interaction [31]. The PEO occlusion in SBA-15 is more apparent than in our earlier studies of MCM-41 as the filler [32].

Melosh et al. [40] have shown that the poly(ethylene oxide)–poly(propylene oxide)–poly(ethylene oxide) (PEO–PPO–PEO) block copolymer acts as a structure-directing agent where the silica cation preferentially associates with PEO blocks. With this composite solid polymer electrolyte, it is significant that the occlusion of polymer improves the miscibility between the organic and inorganic moieties.

The general trends observed for composite polymer electrolytes is not a linear function of the filler concentration [26,33,34,44]. At a low content level, the dilution effect causes specific interactions with the ceramic surface, which promote fast ion transport, and the overall affect enhances the conductivity. On the other hand, at high filler content, the dilution effect predominates and the conductivity decays. In spite of the similarity, the effects described for these systems are different with the composite electrolyte under study here where a majority of lithium is consumed by SBA-15.

In the present composite solid polymer electrolyte, the three kinds of lithium species can be explained in terms of two different conducting mechanisms. The basic ion transport is achieved by random walking through amorphous PEO. A second conduction path is established by lithium-ion hopping in a sequential manner by replacing the nearby vacancies (‘holes’) on the surfaces (both interior and exterior) of the SBA-15 channels. The presence of an additional conducting channel delivers favourable ion conductivity compared with polymers without a SBA-15 composite and exhibits a lower temperature-dependent conductivity (i.e. smaller pseudo activation energy) in the low-temperature region. Nevertheless, a specific interaction of the flexible polymer with the filler surface is essential to promote fast ion transport in the second type of conduction. This conclusion is drawn from the observation that the ion conductivity deteriorates rapidly when phase separations occur. The effect is best illustrated by the difference in ion conductivity during heating and cooling (see Fig. 5(a) and 5(b)). For samples that exhibit good miscibility (below 10 wt.%), the specific interaction becomes stronger by heat-

ing and cooling, and the ion conductivity is higher while cooling. For samples exhibiting phase separation (15 wt.% SBA-15), however, the specific interaction between PEO and SBA-15 is severely affected after melting the polymer, and the ion conductivity increases in first scan but there is no change in the following scan of cooling. Upon cooling below T_c, the PEO is unable to recover its original structure and the ion conductivity becomes larger. Even higher conductivity is noticed on the second heating of a 10 wt.% SBA-15 sample where the stronger coordination between the polymer and SBA-15 acts synergistically for lithium-ion transport. Croce et al. [37] suggested that once the composite electrolytes are annealed at a temperature above the PEO melt; the larger surface area of the added filler prevents local PEO chain reorganization so that a high degree of disorder, is attained at ambient temperature. Annealing creates a large number of thermally-induced defects at the polymer–ceramic interface [19]. These defects accommodate and facilitate movement of lithium ions and impart orders of magnitude increases in conductivity.

Best et al. [45] have discussed nano-composite electrolytes in terms of electrostatic interactions whereby lithium cations will experience a relatively stable potential landscape at the filler surface, i.e. of about the same order as that at the polymer. Lithium ions will then be free to move by segmental motion and activated hopping, with a potential barrier lowered by the filler. The lithium cations form weaker transient bonds with the oxygen atoms of the surface of filler grains during migration, similar to the coordinated transient links they form with the ether oxygen of PEO [46]. This provides extra sites for the cationic transport process, where the bonds between lithium ions and oxygen in the filler surface groups are also subject to breaking and making as with the ether oxygen in the PEO polymer.

The favourable conductivity of the 10 wt.% SBA-15 composite in both the high and low temperature regions is an inherent feature of the combined effect with a remarkable balance of the physical cross-linking, largely suppressed PEO crystallinity and the existence of both types of conducting mechanisms. Most importantly, the mechanical property is sustained even at higher compositions where the mesoporous silica served as both the filler and the tie molecules to improve the adhesion through physical cross-linking with polymer chains.

5. Conclusions

Mesoporous SiO_2 (SBA-15) imparts higher ion conductivity and substantial mechanical strength to a PEO:$LiClO_4$ electrolyte. Solid-state ^{7}Li NMR studies reveal the occlusion of PEO along with lithium ions in the pore channels of the SBA-15. Electron micrographs and DSC studies have shown improved interaction between the polymer and SBA-15 in the presence of a lithium salt. At high SBA-15 content, the conductivity deteriorate due to the development of a SBA-15:Li rich domain and severe phase separation occurs. Annealing above the PEO melting temperature provides more organic–inorganic interaction and prevents PEO recrystallization upon cooling, which results in a further enhancement in ion conductivity. Two types of conduction mechanism occur in this composite electrolyte, namely, lithium ion transport through amorphous PEO, and sequential hopping by replacing the nearby vacancies on the surface (both interior and exterior) of the SBA-15 channels.

Acknowledgements

The authors gratefully acknowledge National Science Council, Taiwan for financial support to perform this work under contract no. NSC. 91-2811-M-008-010.

References

[1] J.R. Mac Callum, C.A. Vincent (Eds.), Polymer Electrolyte Reviews, Elsevier, Amsterdam, 1987.
[2] J.R. Owen, A.L. Laskar, S. Chandra, Superionic Solids and Solid State Electrolytes, Recent Trends, Academic Press, New York, 1989.
[3] B. Scrosati (Ed.), Application of Electroactive Polymers, Chapman & Hall, London, 1993.
[4] M.A. Ratner, A. Nitzman, Faraday Discuss Chem. Soc. 88 (1989) 19.
[5] R. Dupon, B.L. Papke, M.A. Ratner, D.H. Whitmore, D.F. Shriver, J. Am. Chem. Soc. 104 (1982) 6247.
[6] M.M. Doeff, P. Georen, J. Qiao, J. Kerr, L.C. De Jonghe, J. Electro. Chem. Soc. 146 (1999) 2024.
[7] M. Jaipal Reddy, P. Chu, J. Power Sources 109 (2002) 340.
[8] F. Croce, B. Scrosati, J. Power Sources 43 (1993) 43.
[9] X.Q. Yang, H.S. Lee, L. Hanson, J. Mc Breen, Y Okamoto, J. Power Sources 54 (1995) 198.
[10] M. Jaipal Reddy, T. Sreekanth, U.V. Subba Rao, Solid State Ion. 98 (1997) 167.
[11] C.J. Leo, G.V. Subba Rao, B.V.R. Chowdari, Solid State Ion. 148 (2002) 159.
[12] G.B. Appetecchi, F. Croce, M. Mastrogostino, B. Scrosati, F. Soavi, F. Zanelli, J. Electrochem. Soc. 145 (1998) 4133.
[13] F. Croce, G.B. Appetecchi, L. Persi, B. Scrosati, Nature 394 (1998) 456.
[14] F. Croce, L. Persi, F. Ronci, B. Scrosati, Solid State Ion. 135 (2000) 47.
[15] J. Bujdak, E. Hackett, E.P. Gianndis, Chem. Mater. 12 (2000) 2168.
[16] R.A. Vaia, S. Vasudavan, W. Krawiec, L. G Scanlon, E.P. Giannelis, Adv. Mater. 7 (1995) 154.
[17] S. Wong, D.B. Zax, Electrochim. Acta 42 (1997) 3513.
[18] O. Dag, A. Varma, G.A. Ozin, C.T. Kresge, J. Mater. Chem. 9 (1999) 1475.
[19] B. Kumar, L.G. Scanlon, J. Electroceram. 5 (2) (2000) 127.
[20] E. Morales, I. Villarreal, J.L. Acosta, J. Appl. Poly. Sci. 73 (1999) 1023.
[21] G.B. Appetecchi, S. Scaccia, S. Passerini, J. Electrochem. Soc. 147 (2000) 4448.
[22] E. Peeled, D. Golodnitsky, G. Ardel, V. Eshkenazy, Electrochim. Acta 40 (1995) 2197.
[23] V. Di Noto, M. Fauri, M. Vittadello, S. Lavina, S. Biscazzo, Electrochim. Acta 46 (2001) 1587.
[24] W. Wieczorek, J.R. Stevens, Z. Florjanczyk, Solid State Ion. 85 (1996) 67.

[25] S.H. Chung, Y. Wang, L. Persi, F. Croce, S.G. Greenbaum, B. Scrosati, E. Plichta, J. Power Sources 97–98 (2001) 644.
[26] F. Croce, L. Persi, B. Scrosati, F. Serriano-Fiory, E. Plichta, M.A. Hendrickson, Electrochim. Acta 46 (2001) 2457.
[27] D. Zhao, Q.Huo.J. Feng, B.F. Chmelka, G.D. Stucky, J. Am. Chem. Soc. 120 (1998) 6024.
[28] Z. Luan, M. Hartmann, D. Zhao, W. Zhou, L. Kevan, Chem. Mater. 11 (1999) 1621.
[29] Z. Luan, E.M. Maes, P.A.W. Vander Heide, D. Zhao, R.S. Czernuszewicz, L. Kevan, Chem. Mater. 11 (1999) 3680.
[30] Z. Luan, J.Y. Bae, L. Kevan, Chem. Mater. 12 (2000) 3202.
[31] M. Imperor-Clerc, P. Davidson, A. Davidson, J. Am. Chem. Soc. 122 (2000) 11925.
[32] P. Chu, M. Jaipal Reddy, H.M. Kao, Solid State Ion. 156 (2003) 141.
[33] H.Y. Sun, Y. Takeda, N. Imanishi, O. Yamamoto, H.J. Sohn, J. Electro. Chem. Soc. 147 (2000) 2462.
[34] S.A. Hashmi, A.K. Thakur, H.M. Upadhyaya, Eur. Poly. J. 34 (1998) 1277.
[35] T. Sreekanth, M. Jaipal Reddy, S. Ramalingaiah, U.V. Subba Rao, J. Power Sources 79 (1999) 105.
[36] S.A. Hashmi, A. Kumar, K.K. Maurya, S. Chandra, J. Phys. D Appl. Phys. 23 (1990) 1307.
[37] F. Croce, R. Curini, A. Martinelli, L. Persi, F. Ronci, B. Scrosati, R. Caminiti, J. Phys. Chem. B 103 (1999) 10632.
[38] M. Jaipal Reddy, P. Chu, Electrochim. Acta 47 (2002) 1189.
[39] M. Jaipal Reddy, P. Chu, Solid State Ion. 149 (2002) 115.
[40] N.A. Melosh, P. Lipic, F.S. Bates, F. Wudl, G.D. Stucky, G.H. Fredrickson, B.F. Chmelka, Macromolecules 32 (1999) 4332.
[41] J. Przyluski, M. Siekierski, W. Wiezorek, Electrochim. Acta 40 (1995) 2101.
[42] W. Wiezorek, Z. Florjancyk, J.R. Stevens, Electrochim. Acta 40 (1995) 2251.
[43] S. Wong, R.A. Vaia, E.P. Giannelis, D.B. Zax, Solid State Ion. 86–88 (1996) 547.
[44] Z. Wen, T. Itoh, M. Ikeda, N. Hirata, M. Kubo, O. Yamamoto, J. Power Sources 90 (2000) 20.
[45] A.S. Best, J. Adebahr, P. Jacobsson, D.R. MacFarlane, M. Forsyth, Macromolecules 34 (2001) 4549.
[46] P.A.R.D. Jayathilaka, M.A.K.L. Dissanayake, I. Albinsson, B.E. Mellander, Electrochim. Acta 47 (2002) 3257.